



Humanoid Robot Locomotion Planning and Control

Exploring the Effects of Center of Mass Height
Variation

B.J. van Hofslot

Literature Survey



Humanoid Robot Locomotion Planning and Control

Exploring the Effects of Center of Mass Height Variation

LITERATURE SURVEY

B.J. van Hofslot

August 9, 2018



The work in this survey was supported by the Institute for Human and Machine Cognition.
Their cooperation is hereby gratefully acknowledged.



Copyright © Cognitive Robotics
All rights reserved.



Abstract

In this survey relevant literature to humanoid robot locomotion planning and control is analyzed and discussed. First, a study is done on the terminology and simplified models used in humanoid robotics. After this, a global exploration of the current most popular planning and control strategies is done and summarized. An entire chapter is dedicated to the current attempts to use height variation in control and planning of locomotion. It appears that there are some attempts in this, but not many, and that hardware results are not often shown. This explains the research of focus and the challenge to apply it on hardware: the effects of Center of Mass (CoM) height variations in planning and control of humanoid robot locomotion.

Table of Contents

1	Introduction	1
1-1	Motivation	1
1-2	Objective	2
2	Modeling & Terminology	3
2-1	Walking Terminology	3
2-1-1	Single support phase	3
2-1-2	Double support phase	3
2-2	Full Robot Model	4
2-2-1	Current bipedal robots	4
2-2-2	Modeling	4
2-2-3	Simulation	5
2-3	Linear Inverted Pendulum (LIP) Models	5
2-3-1	Conservation of LIP Orbital Energy (E_{LIP})	6
2-3-2	The Instantaneous Capture Point (ICP)	6
2-4	Humanoid Robot Terminology	7
2-4-1	The Center of Pressure (CoP)	7
2-4-2	The Zero Moment Point (ZMP)	8
2-4-3	The Centroidal Momentum Pivot (CMP)	8
2-4-4	Linear momentum rate	8
2-4-5	Other points	9
2-5	Analysis & Discussion	9

3 Planning, Control & State Estimation	11
3-1 Planning	11
3-1-1 Footstep planning	11
3-1-2 Dynamic planning	12
3-1-3 Swing leg trajectories	12
3-2 Control	12
3-2-1 High level control	13
3-2-2 Mid and low level control	13
3-2-3 Compliant control	13
3-3 State Estimation	14
3-4 Analysis & Discussion	14
4 Varying CoM Height	15
4-1 Orbital Energy for Nonlinear CoM Trajectories	15
4-2 Divergent Component of Motion (DCM) for Varying Height	16
4-3 Other Approaches	17
4-4 Trajectory Optimization for Nonlinear Systems	18
4-5 Analysis & Discussion	18
5 Conclusion	21
Bibliography	23
Glossary	27
List of Acronyms	27
List of Symbols	28

List of Figures

1-1	Three-Dimensional Space (3D) motion of LIP model with foot at the base and a mass with inertia at the tip. The CoM moves at constant height.	2
2-1	A selection of currently popular humanoid robots. (a) Boston Dynamics' new Atlas [1]. (b) Previous version of Atlas [2] and (c) NASA's Valkyrie [3] walking over rough terrain at IHMC. (d) ATRIAS, a bipedal robot [4].	4
2-2	3D motion of LIP model.	5
2-3	Visualization of path and states by the capture of the point mass according ICP theory.	6
2-4	3D motion of LIP model with foot. The yellow cross points out the CoP location.	7
2-5	3D motion of LIP model with foot and body inertia. The blue cross points out the CMP location.	9
3-1	Valkyrie walking in Simulation Construction Set (SCS). In the left window a footstep plan is made visible together with the swing leg trajectories with their knot points. The red arrow indicates the ground reaction wrench and the window on the right displays the current ground contact with some reference and measured points.	12
3-2	Overview of control framework used at IHMC, retrieved from [5]	14
4-1	Nonlinear simplified system in Two-Dimensional Space (2D).	16

Chapter 1

Introduction

There are many situations in the world which are not safe, where a human is sent to help. Exploring the terrains of nuclear disasters, searching in a house on fire and clearing mine fields are all examples of this. Technology has extended the humans' hand through history to a point where nowadays some people are wondering if we have almost hit the limits of fishing Mother Nature's pond of technology. Safety standards in both professional and personal environments have greatly improved with the help of knowledge and technology. As is noticeable from the videos of Boston Dynamics going viral all over the world, legged robots, and more specifically humanoid robots, become more in a developed stage. However, comparing with the human physical capabilities, humanoid robots are still at most in a child phase. The usefulness of these devices and the growth opportunities are a clear motivation to improve them.

1-1 Motivation

The walking humanoid robot system is highly complex. It deals with nonlinear multibody dynamics, complex kinematics, hybrid dynamics between switching ground contacts, unilateral friction-limited contact constraints and actuation limitations. Past research has approached nonlinearities with a linearized description of a walking robot [6, 7, 8] and has tackled joint level complexities with separating high level and joint level control [9, 5]. The planning problem of a walking gait has often been tackled by separating the footstep plan from the body motion plan [10, 11, 12]. Although all these methods break the complexity of the system down and give a better approximation of how it will behave dynamically, often still a lot of assumptions are made. Linearization of the model has the advantage to give a relatively simple measure, that can have a closed form solution in planning problems and can be used in linear control. In Figure 1-1 the basic model that is often considered is shown. The robot is modeled as a Linear Inverted Pendulum (LIP) with constant height, were the foot and body inertia can be used for control. Recently research has been done in taking the constant height assumption away [13, 14, 15, 16, 17], but application of varying height models in control and planning is not yet proven to be successful.

1-2 Objective

In this literature survey, the focus is to find how Center of Mass (CoM) height variations are used in planning and control of a bipedal robot, with the goal of improving the dynamical behavior over rough, but also flat, terrain and improving robustness properties against disturbances. Even though this is the research area of focus, a global study is done on humanoid robotics research in general, as it is important to understand what strategies are used in aspects that are related to the problem.

In Chapter 2, a brief overview is given of the basic humanoid walking related models and terminology. In Chapter 3, a general review is conducted on the current planning, control and state estimation strategies in humanoid robotics. Special attention is given to papers that were applied to Boston Dynamics' Atlas or NASA's Valkyrie at IHMC, as research is conducted and hopefully applied at this institute. In Chapter 4, a full in-depth study is performed on publications that address CoM height variation directly. In Chapter 5, there is concluded on the overall literature study. Information and ideas from different publications are tied together to attempt to formulate a balanced insight in the possibilities and concerns to tackle the problem.

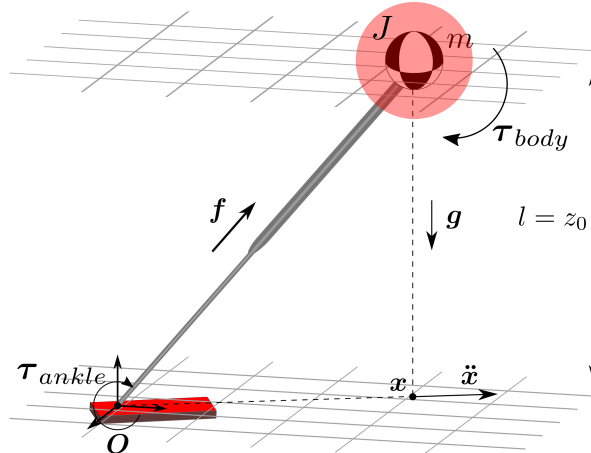


Figure 1-1: Three-Dimensional Space (3D) motion of LIP model with foot at the base and a mass with inertia at the tip. The CoM moves at constant height.

Chapter 2

Modeling & Terminology

As the design of humanoid robots is based on that of a human being, a lot of terms and models used by roboticists and human motion researchers overlap. In this chapter, an overview is given of an important part of the fundamental naming and theory that is used for the system behavior and description of a humanoid robot.

2-1 Walking Terminology

There are a variety of terms used in describing walking or locomotion. In this section, the terminology in this report is determined, which is also widely used, as for example can be found in [18].

2-1-1 Single support phase

During the single support phase, the biped is only with one foot on the ground. The other foot is swinging through the air without ground contact, in the process of taking a step. The leg in contact with the ground is called the *stance leg* and the leg taking a step is called the *swing leg*. In a simplified walking model the single support phase with hybrid switching between contacts is often the only phase considered. There exist also bipedal robots with only this phase applied on hardware, like ATRIAS from Oregon State University [19]. This robot however, by the point-foot support with only the single stance leg per single support phase, has to keep stepping without interruption to stay stable, as the unstable equilibrium above the foot diverges quickly.

2-1-2 Double support phase

In more human-like walking, next to the single support phase the double support phase is considered, also called the transfer phase in some cases. This is the phase during walking where both feet are on the ground.

2-2 Full Robot Model

The human body is a very complex system and has redundant joints and actuation. Among those joints exist joints with one degree of freedom, like the knee joint, but also joints with multiple degrees of freedom, like the hip joint for example. Reproducing this in robotics is a challenging task and different choices can be made in the complexity of the system and the type of actuators.

2-2-1 Current bipedal robots

In Figure 2-1 a couple of modern bipedal robots are displayed. Figure 2-1a displays the newest model of Boston Dynamics' Atlas, a device that impressed a lot of people with its capabilities. It can run, stand up again after it has fallen over and it can even do a backflip, as shown in videos. Those are all incredible improvements with respect to earlier achieved results in humanoid robotics. Figure 2-1b shows the previous Atlas model. This robot is used by IHMC to compete in the DARPA Robotics Challenge [20] and it gets still used to test new features on. Figure 2-1c shows the Valkyrie humanoid robot [21], which is built by NASA. A version of this robot is also at IHMC. A difference between the Atlas robots and Valkyrie, is that the both Atlas versions are controlled with hydraulic actuation. Valkyrie makes use of so called series elastic actuators. Figure 2-1d shows the ATRIAS robot from Oregon State University [19]. This is a good example of a, compared to the previous three examples, relatively more simple model. It has point feet and no arms for manipulation. In this report this is therefore defined as a bipedal robot, but not as a humanoid.

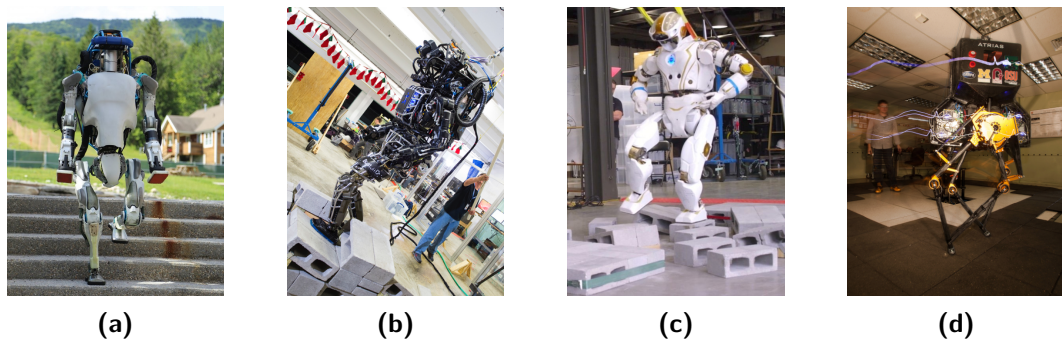


Figure 2-1: A selection of currently popular humanoid robots. **(a)** Boston Dynamics' new Atlas [1]. **(b)** Previous version of Atlas [2] and **(c)** NASA's Valkyrie [3] walking over rough terrain at IHMC. **(d)** ATRIAS, a bipedal robot [4].

2-2-2 Modeling

As can be seen from the images in Figure 2-1, a lot of bipedal robots are capable of more tasks than walking alone. As this survey is focused on walking and stabilizing by the legs, tasks as for example grasping and having environment contact of the upper body are not considered. However, even without contact the upper body plays a crucial role in the dynamics of the robot. Chest and arm movements can create angular momentum that can control the system,

which is considered in this survey. An example of the modeling of a full robot in joints and links can be found in [22].

2-2-3 Simulation

Because of the complexity and size of the systems considered, simulation is key. There exist multiple simulation environments, from which one of them is the open source Gazebo [23]. At IHMC an inhouse developed simulation environment is used: Simulation Construction Set (SCS). This environment is written in Java.

2-3 Linear Inverted Pendulum (LIP) Models

In modeling of walking, one of the most important assumptions often made is the modeling of the stance leg as a LIP, as for example in [24]. Besides this, a not-linearized inverted pendulum is also widely used in the modeling of walking [25]. For planning and control however, a linearized description is desirable. In the Two-Dimensional Space (2D) LIP equations of motion

$$\ddot{x} = \frac{g}{l}x \quad (2-1)$$

where l is the pendulum length and x the Cartesian x-coordinate of the pendulum tip, the motion of the tip along the x-axis does not affect l . At any position x , a local virtual straight pendulum can be considered, so this motion is at a constant height and $l = z_0$ holds. As in Three-Dimensional Space (3D) by the linear model the system dynamics can be decoupled, the dynamics in y -direction will read the same: $\ddot{y} = \frac{g}{l}y$. In Figure 2-2 this motion is visualized if the Center of Mass (CoM) is relatively far from from the base. The pendulum base lies in the origin and $\mathbf{x} = [x, y]^T$ is the 2D CoM projection on the horizontal plane. Because the LIP assumption holds, the vertical component of the leg force \mathbf{f} has to cancel out gravity acceleration: $f_z = mg$.

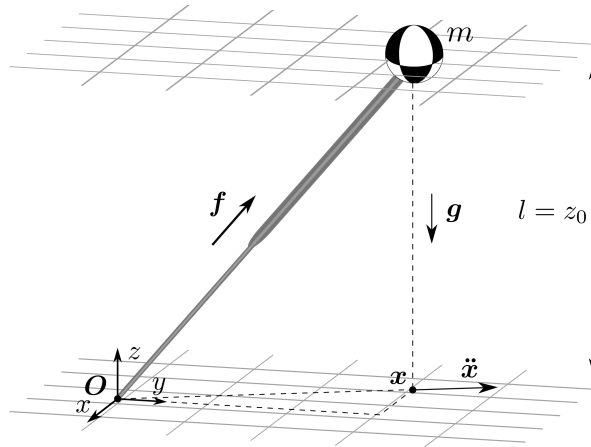


Figure 2-2: 3D motion of LIP model.

2-3-1 Conservation of LIP Orbital Energy (E_{LIP})

[6] had a crucial finding in an extended use of LIP models. Because $F = ma$, $I = Fv$ and $E = Fs = \int Fvdt$, there can be reasoned that if one takes the time integral of the product of the second and the first derivative of a state, an expression for a normalized energy can be achieved: $\frac{E}{m} = \int avdt$. In the mentioned publication that same action is applied on Eq. (2-1):

$$\int (\ddot{x} - \frac{g}{l}x)\dot{x}dt = \frac{1}{2}\dot{x}^2 - \frac{g}{2z_0}x + C = 0 \quad (2-2)$$

with C the integration constant. The LIP Orbital Energy is defined as $E_{LIP} = -C$.

2-3-2 The Instantaneous Capture Point (ICP)

Although the finding of the LIP Orbital Energy was very important for future robot motion modeling, more than a decade later [7] introduced the Capture Point (CP). Taking $E_{LIP} = 0$ and taking the square root of Eq. (2-2) gives

$$x_{CP} = \sqrt{\frac{z_0}{g}}\dot{x} \quad (2-3)$$

where x_{CP} is the CP, measured from the current pendulum tip position, based on the current tip velocity \dot{x} . This is the point where the velocity is driven to zero and the pendulum is upright. In Figure 2-3 a 2D visual explanation is given of this point. Later, the ICP was

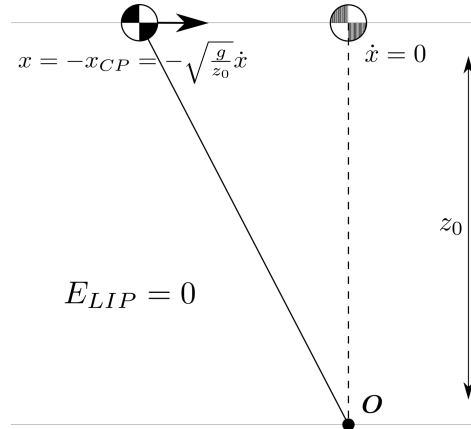


Figure 2-3: Visualization of path and states by the capture of the point mass according ICP theory.

introduced [8], which gives a slightly different description of the point:

$$x_{ICP} = x + \sqrt{\frac{z_0}{g}}\dot{x} \quad (2-4)$$

where x_{ICP} is the ICP. In this way, the point can be described in the environment coordinates. The x - and y coordinate can be decoupled as in the equation of motion of Eq. (2-1). However, in the 2D horizontal plane it is not guaranteed that the velocity direction of the CoM is towards the ankle point.

ICP dynamics

Because the ankle is not always located at the same location as the ICP for the current horizontal velocity, for modeling and planning the time derivative is taken of the ICP, which is named the ICP dynamics [8]. This time derivative can be written as a function of the current ICP location:

$$\dot{\mathbf{x}}_{ICP} = \sqrt{\frac{g}{z_0}} \mathbf{x}_{ICP} \quad (2-5)$$

where \mathbf{x}_{ICP} is the xy -vector of the ICP location and assuming that the pendulum base is the origin.

2-4 Humanoid Robot Terminology

As the ICP is a measure for the behavior of a bipedal robot, there exist plenty of terms and descriptions for specific virtual points and forces on and acting on the robot. In this section a short summary is given from the most popular jargon.

2-4-1 The Center of Pressure (CoP)

The larger feet of a human than those of a dog make him more capable of upright walking, due to an increase of controllability of the modeled-as-LIP human. The ankles can apply a torque that would virtually move the position of the base of the inverted pendulum, so that the linear acceleration on the CoM as in Eq. (2-1) and the capture point as in Eq. (2-5) change. The new virtual base is called the CoP. By its definition, this point only lives within the foot polygon [26]. In Figure 2-4 the definition of the CoP is visualized. If the point mass is restricted to move on a constant height, the vertical component of \mathbf{f}' counteracts gravity: $f'_z = g$.

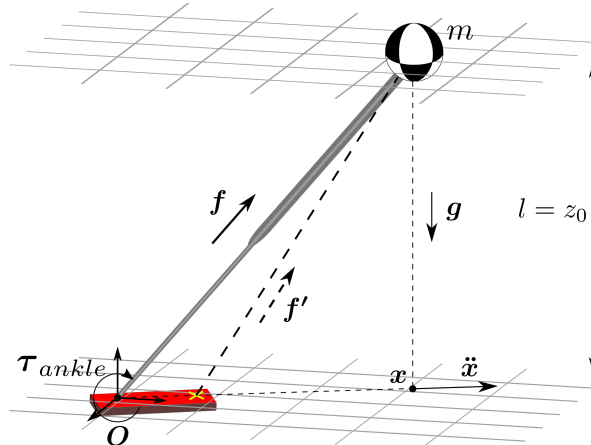


Figure 2-4: 3D motion of LIP model with foot. The yellow cross points out the CoP location.

2-4-2 The Zero Moment Point (ZMP)

The ZMP coincides during stable walking with the CoP, like described in [26]. The two points however are not equal in unstable or more complicated cases, like falling over. The CoP is restricted to be in the foot polygon, as this is a point that links to contact forces [27]. The ZMP however is not restricted to lie within the foot polygon. The ZMP is the point on the ground where the tipping moment equals zero. The tipping moment is defined as the component of the moment that is tangential to the ground surface. The ZMP initially was introduced in [28].

2-4-3 The Centroidal Momentum Pivot (CMP)

The earlier mentioned points give sufficient measure for a LIP model with point mass and finite sized feet. However, any angular momentum applied by the body does not affect those points. In the case of the CoP for example, the model assumes the resulting reacting force acts from the CoP through the CoM. The CMP takes angular momentum into account, which can be used as a measure and for control [29]. This is defined as the point where a line passing through the CoM, parallel to the ground reaction force intersects with the ground surface. The CMP is defined as

$$x_{CMP} = x_{ZMP} + \frac{\tau_{y,CoM}}{F_{gr,z}} \quad (2-6)$$

$$y_{CMP} = y_{ZMP} - \frac{\tau_{x,CoM}}{F_{gr,z}} \quad (2-7)$$

where τ_{CoM} is the torque around the CoM, $[x_{ZMP}, y_{ZMP}]$ the ZMP location on the horizontal plane and $F_{gr,z}$ is the ground reaction force in z-direction in Cartesian space. In Figure 2-5 it is displayed how the body angular momentum affects the ground reaction force \mathbf{f}' from the CoP and how the CMP can be determined with the intersection of a parallel line through the CoM and the ground plane. For clarity the point in the image lies on the line from \mathbf{O} to \mathbf{x} . This has not to be the case however, as the body can exert angular momentum along all axes.

2-4-4 Linear momentum rate

To combine the effects described in this section in one single measure, often the linear momentum or linear momentum rate is considered in the horizontal plane. This boils down to be a combination of the LIP equations of motion and the CoP, ZMP or CMP. Using the CMP the linear momentum rate is then defined as

$$\dot{\mathbf{i}} = m\ddot{\mathbf{x}} = m\frac{g}{z}(\mathbf{x} - \mathbf{x}_{CMP}) \quad (2-8)$$

where $\dot{\mathbf{i}}$ is the linear momentum rate in the horizontal plane, \mathbf{x} the 2D CoM position and \mathbf{x}_{CMP} the CMP position.

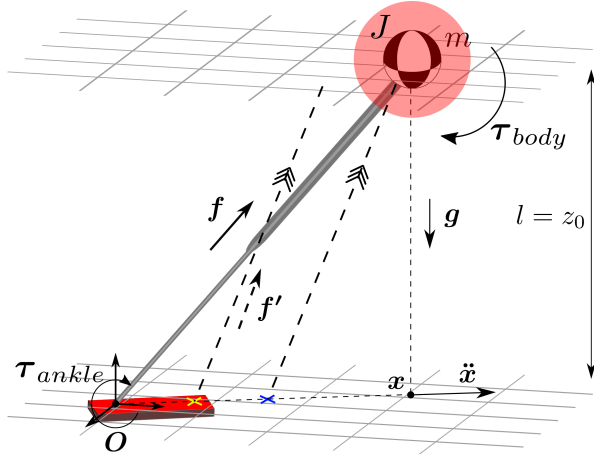


Figure 2-5: 3D motion of LIP model with foot and body inertia. The blue cross points out the CMP location.

2-4-5 Other points

Other than the points mentioned before, there are sometimes other points considered in humanoid robotics. Examples of this are the enhanced Centroidal Momentum Pivot (eCMP) and the Virtual Repellent Point (VRP) [30], but those are not further discussed here.

2-5 Analysis & Discussion

From the study in this chapter it becomes clear that oftentimes the complex system of a walking robot is captured in a relatively simple model, namely that of a LIP with a mass with inertia on the tip and a base that is maneuverable within limits. The combined dynamics of this configuration define the dynamics in the horizontal plane of the LIP. This however requires the nominal ground reaction force to have a vertical component equal to the force applied by gravity. For motion over a flat surface, it seems intuitively as a desirable goal to have a constant height. If the goal is to move somewhere in the planar world, height variation and thus height acceleration would only waste energy. However, for having a walking motion where the gravity vector is not perpendicular to it, the assumption of the constant force in vertical direction might not be a solid assumption. Even on a flat surface the CoM varies slightly in height [31]. Moreover, varying leg force could be used to accelerate or stop quicker, which would mean a different force is applied than assumed in the LIP model. The different leg force changes the horizontal component of the force, which can control the motion. This also results in a change of its vertical component, which after time changes the CoM height, as it is not equal to gravitational forces anymore.

Chapter 3

Planning, Control & State Estimation

In this chapter the most common planning, control and state estimation strategies are pointed out and reviewed. As mentioned before, publications that regard the humanoid robots in use at IHMC, get special consideration.

3-1 Planning

In robotics, the planning problem can be described with a desired final goal of the motion, constraints on the path itself as terrain where collision needs to be avoided and constraints on the capabilities of the system as kinematic limits and actuation limits. As the dynamics of a humanoid robot are complex and underactuated, there exist numerous ways to generate a walking plan. This typically ranges from reactive stepping and tracking a desired velocity to precise foot placements. In this section common planning strategies are described.

3-1-1 Footstep planning

While not all bipedal robots require a footstep plan to walk, most humanoids do. A footstep plan is a sequence of foothold references on the ground. Those can be computed either offline or online. Offline, either an autonomous planner can make a plan, or a robot operator can define desired footsteps manually. Online the robot in some cases can re-plan to avoid collision or adjust a footstep to use for stabilization. In [10] is described how an online plan can be generated as an example. At IHMC, based on LiDAR terrain information from the robot's head, the operator can define footholds which in the Graphical User Interface (GUI) turn green or red for kinematic reachability. There is also work on algorithms to adjust steps real-time for stability [32] and autonomous planners based on for example the A* algorithm. As footstep planning can be decoupled from the varying height problem, the footstep plan is assumed to be given beforehand in this survey.

3-1-2 Dynamic planning

Through the history of humanoid robots, there are various strategies used to generate a body path plan. There are differences in planning in joint-space and planning only a Center of Mass (CoM), Center of Pressure (CoP) or Instantaneous Capture Point (ICP) trajectory for example. This is greatly depending on the control strategy that is used, but also on the complexity of the robot. Currently at IHMC an ICP plan is generated based on a footstep plan with CoP knot points [12]. Based on the desired time of the footstep plan, the ICP dynamics are integrated backwards in time to come to a reference trajectory. This plan is tracked using PD-control, where the Centroidal Momentum Pivot (CMP) is used as control input to achieve the desired ICP plan. During the double support phase the Linear Inverted Pendulum (LIP) assumption is not valid, and the ICP trajectory is here moved between two footsteps by a time polynomial.

3-1-3 Swing leg trajectories

If the robot places its foot from the current footprint to the next, a more local plan is generated. This is often done by defining a polynomial spline from the one foothold to the other, with knot points at a certain height above the ground to make the foot not hit the ground. This spline can be generated as a set of piece-wise minimum jerk trajectories. The minimum jerk trajectory minimizes the jerk, the third derivative of position with respect to time, and needs a desired completion time for the trajectory as input. This desired time for the entire spline is called the desired swing time for this step. In Figure 3-1 swing leg trajectories are displayed in the simulation environment of Simulation Construction Set (SCS), together with among other things a footstep plan.

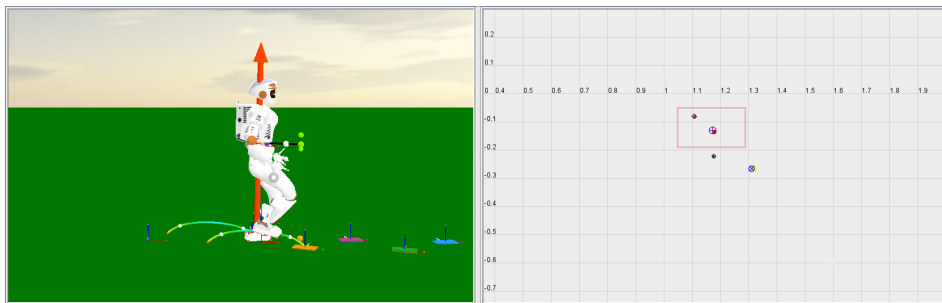


Figure 3-1: Valkyrie walking in SCS. In the left window a footstep plan is made visible together with the swing leg trajectories with their knot points. The red arrow indicates the ground reaction wrench and the window on the right displays the current ground contact with some reference and measured points.

3-2 Control

To track a generated high level plan the system has to be controlled. PID-control, LQR and MPC are all used in humanoid robotics. Again, there are differences in joint-level control and for example the control of the desired CoM position, which often are separated in high level

and low level control. In some cases, like with the Hybrid Zero Dynamics (HZD) approach as described in [33], there is no decoupling between such levels. However, the HZD is for this reason often applied to simpler robots, as in the mentioned paper and on ATRIAS. Furthermore, the HZD approach is designed for systems with a degree of underactuation of one, which corresponds more to a Two-Dimensional Space (2D) than a Three-Dimensional Space (3D) robot model.

3-2-1 High level control

Tracking the ICP trajectory as is done at IHMC is an example of high level control. The robot in this stage can be seen as a LIP with a finite sized foot and body angular momentum. At a current footstep, using the right combination of ankle torque and angular momentum, the robots motion can in theory be controlled considering the simplified LIP model. The robot is assumed to keep itself at a constant height and expected to generate the desired centroidal momentum. Simplification of the model to only a CoM, angular momentum and a ground reaction force, makes control more accessible than looking at joint level. The desired values of the high level controller are send to a mid level controller to translate this information to joint level control.

3-2-2 Mid and low level control

As the real robot is not a LIP and cannot generate high level control inputs as angular momentum as a single control input, other layers of control are needed: mid and low level control. Low level controllers are often based on inverse kinematics and inverse dynamics. This concept is also widely used in industrial robotic manipulators, as for example in [34]. What often the basis is for desired motions on joint scale is the fact that so called centroidal dynamics about the pelvis or CoM have to equal the wrenches applied on the environment, as for example in [35] and [5]. An important constraint on wrenches applicable on the environment is the unilaterality of the contact and the available contact friction. This is often captured in having a so called wrench cone above the foot, wherein the resulting ground wrench has to lie. The centroidal dynamics are a combination of the linear and angular momentum rate. In Figure 3-2 an overview of the controller structure at IHMC is given. The momentum rate of change objective consist during walking mainly of the linear momentum rate as in Eq. (2-8). The motion tasks are for example moving the swing leg. This information from the high level controller is then translated in a quadratic program, that defines the solution as a set of joint accelerations and reaction wrenches. This is translated to joint level with inverse dynamics.

3-2-3 Compliant control

In the walking of a bipedal robot with legs hybrid switching between swing and stance, a problem gets introduced with this hybrid phase shift. During swing, a trajectory is tracked using a control strategy that links more to position tracking. When the foot hits the ground, it switches instantly to the stance phase, where its position is fixed and its control actions are mainly based on forces. This instant switch can cause instabilities in the controller and an agile, compliant control strategy is needed. In [36] is described how for different phases a

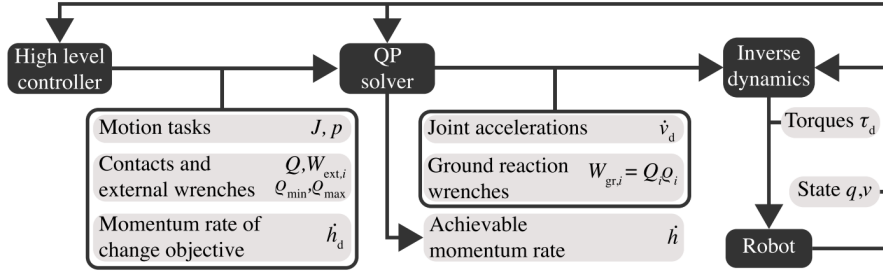


Figure 3-2: Overview of control framework used at IHMC, retrieved from [5]

different set of controller gains can be used to deal with the difference of impedance needed in control.

3-3 State Estimation

As state estimation is dependent on the available sensor data and the quality of the data, the possible strategies for estimation depend on the particular robot model. Typically, the robot has position sensing in all joints, that sometimes have torque sensing as well. An Inertial Measurement Unit (IMU) can be present in the body, or even in some body parts. State estimation of for example the pelvis orientation and velocity can be done by combining sensor data from both the body IMU and an inverse dynamics algorithm that uses information from joints. On joint level, a low-pass filter can be applied and then based on the dynamics of the robot, a heuristic approach in combining the IMU and joint data can be used to estimate the pelvis state, as is done in [5]. Another possibility is the use of more sophisticated sensor fusing techniques as the Extended Kalman Filter (EKF), as in [9]. Due to the complexity of the system this can be however challenging, especially with application on hardware.

3-4 Analysis & Discussion

The entire framework to plan and control the motion of a humanoid robot is so extensive, that it is important to narrow the areas of focus. The knowledge gained from the investigation for this chapter gives a good basis of understanding what the current bottle necks in humanoid robot control and planning are. The current frameworks do not regard any height variation of the inverted pendulum model most of the times, which of course is not done without reasons. First, a linearized model is very desirable in control, as the computational cost of such is much lower than with nonlinear ones. Second, with the linear model a plan through the 3D world can by dynamics mostly captured in a 2D plan, which simplifies the planning problem a lot.

For a varying height model the computation time might be an important aspect, especially for control and online planning, as full pendulum or robot dynamics are nonlinear. This has to be taken into consideration.

Chapter 4

Varying CoM Height

As mentioned earlier, recently work has been done in removing the constant height assumption from the walking model. The motivation for this is threefold. The use of height can be used in tracking control. Where angular momentum and the Center of Pressure (CoP) are often the two control inputs for a Linear Inverted Pendulum (LIP) model of the current swing phase, the use of height, thus a varying leg force, can be used as a third input. Furthermore, in motion over un-flat terrain a varying height model can give a better approximation of how the dynamics will behave over time. Even over flat terrain, the Center of Mass (CoM) trajectory of a human does not follow a straight line, where the dynamic behavior differs from the LIP assumption. In other words: both control and planning can be improved.

Before there is looked at different approaches, a system description for a Two-Dimensional Space (2D) inverted pendulum with a point mass on the tip with varying length is defined. Because the force the pendulum applies on the point mass does not have to be equal to the gravitational acceleration in its vertical component, the system can be described as a traveling point mass subject to a force coming from a point on the ground. This is visualized in Figure 4-1.

The non-linear model of a traveling CoM subject to a force coming from the $[0, 0]$ point on the ground is for the 2D xz -plane

$$m\ddot{x} = F \frac{x}{\sqrt{x^2 + z^2}} \quad (4-1)$$

$$m\ddot{z} = -mg + F \frac{z}{\sqrt{x^2 + z^2}} \quad (4-2)$$

where $F = \|\mathbf{f}\|$ is the leg or ground reaction force and $[x, z]$ the position of the point mass.

4-1 Orbital Energy for Nonlinear CoM Trajectories

The nonlinear equations of motion of Eq. (4-2) are used in [37]. The authors constrain $z = f(x)$ and integrate the equations of motion over time, how a similar conservation of

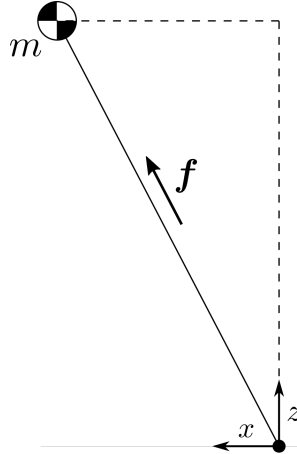


Figure 4-1: Nonlinear simplified system in 2D.

orbital energy as in Eq. (2-2) is derived. This orbital energy however is not required to be a straight line trajectory, but depends on the function $f(x)$. The full integration can be found in the paper, but the final expression writes as

$$E_{\text{orbit}} = \frac{1}{2} \dot{x}^2 \bar{f}^2(x) + g x^2 f(x) - 3g \int_{x_0}^x f(\xi) \xi d\xi = \frac{1}{2} \dot{x}_0^2 \bar{f}^2(x_0) + g x_0^2 f(x_0). \quad (4-3)$$

where $\bar{f}(x) = f(x) - f'(x)x$, $[x_0, \dot{x}_0]$ is the initial horizontal state and velocity and $[x, \dot{x}]$ is the current horizontal state and velocity. There is experimented in simulation with a symmetric polynomial, where the trajectory is tracked using a PD feedback scheme where the leg force is the control input. The polynomial description makes the integral directly solvable, based on the initial and current state. To make a clear separation between LIP Orbital Energy (E_{LIP}), this energy form will be defined in this report as Nonlinear Orbital Energy (E_{orbit}).

Recently, this is used in a Model Predictive Control (MPC) formulation and basic simulations have been done in [14]. The main idea in this paper is to define four constraints on the trajectory $f(x)$, which define the four constants of a cubic polynomial by a matrix inversion. Those consist of two constraints on the initial conditions, one constraint on the final condition and one constraint on the conservation of E_{orbit} . The matrix inversion is done offline, so that the control input can directly be written as a function of the polynomial constants and thus as a function of the initial and final states.

4-2 Divergent Component of Motion (DCM) for Varying Height

A couple of attempts in the use of varying height are found in adaptations of the Instantaneous Capture Point (ICP). A couple of variations on the Divergent Component of Motion (DCM) are examples of this. There exist multiple definitions of this DCM and for clarity different mentions are explained and compared, as some of them seem to be interesting with respect to height usage. For simplicity and comparability, in all coming equations the mentions of CoP and Zero Moment Point (ZMP) in the publications are set to zero. In [38] the DCM is defined as

$$q = x + \frac{1}{\omega_0} \dot{x} \quad (4-4)$$

based on a LIP model, where $[x, \dot{x}]$ is the CoM position and velocity and q is the DCM. Thus, this point is the same as the ICP from Eq. (2-5) plus the CoM horizontal location.

In [30] the DCM is defined as a Three-Dimensional Space (3D) point. This is used in a un-even terrain path planner. The DCM is here defined as

$$\xi = x + b\dot{x} \quad (4-5)$$

where $\xi = [\xi_x, \xi_y, \xi_z]^T$ is the DCM, $x = [x_{CoM}, y_{CoM}, z_{CoM}]^T$ and $\dot{x} = [\dot{x}_{CoM}, \dot{y}_{CoM}, \dot{z}_{CoM}]^T$ are the CoM position and velocity and $b > 0$ is the time-constant of the DCM dynamics.

[13] uses this and defines the constant $b = 1/\omega_0$, where $\omega_0 = \sqrt{\frac{g}{z_{CoM}}}$. This makes it again the same as the ICP, but with a z component in the state. The DCM is derived with respect to time, where ω is posed to be time varying, so the height is time varying. This brings a new expression and is called the time varying DCM, where the derivative is written as

$$\dot{\xi} = (1 - \frac{\dot{\omega}}{\omega^2})\dot{x} + \frac{1}{\omega}\ddot{x} \quad (4-6)$$

where ω is the so called time varying natural frequency of the inverted pendulum.

[17] mentions it uses the DCM from Takenaka et al. and writes this as

$$\xi(t) = \dot{c}(t) + \omega(t)c(t) \quad (4-7)$$

if the CoP vectors are set to zero, where $[c, \dot{c}]$ is the 3D CoM position and velocity and ξ is the 3D DCM. This is used in a MPC scheme to capture the inverted pendulum CoM. There is stated that if ω is not time varying, $\omega = \sqrt{\frac{g}{z}}$ holds. As is stated in the paper that the DCM of Eq. (4-7) is a velocity rather than a point, this is equal to the time derivative of Eq. (4-5).

4-3 Other Approaches

Besides derivations of the ICP for varying height and the E_{orbit} , there are other approaches that describe the effects of varying height. The authors of [15] come up with different strategies to use varying height to generate impact or to relatively speed up the CoM motion compared to the ICP trajectory. Besides gravity, an extra vertical acceleration constant is added in the LIP equations of motion.

In [39] a so called Spring-Loaded Inverted Pendulum (SLIP) model is used to deal with height variation on a humanoid robot. The SLIP model lets the pendulum behave like a spring, where a control gain k accounts for the ‘stiffness’ of the spring. Trajectories are generated using an optimization program.

An applied approach is described in [16]. For different step lengths and step heights, trajectories are generated offline using a direct collocation optimization framework. Online is interpolated between trajectories with knowledge of the current step and the upcoming step. The trajectories are on joint level and make use of the earlier discussed Hybrid Zero Dynamics (HZD) approach. This is applied on hardware, but with the sagittal motion supported and thus only the 2D dynamics in the xz -plane are considered. Interesting is that the different trajectories correspond with different step timings, which is not always implemented in humanoid robot motion planning.

In [40] is an extensive method described to generate a motion plan for nonlinear systems. In

an algorithm, Lyapunov functions of local linearizations of the nonlinear model are evaluated, from which a feasible trajectory is derived. The main idea is that with the Lyapunov functions a measure of convergence of the local system can be proved. From a set of regions defined by converging functions, a feasible trajectory can be selected. Experiments are done on an inverted pendulum, generating trajectories for the swing-up task.

4-4 Trajectory Optimization for Nonlinear Systems

As becomes clear, looking at the simplified varying height robot model, nonlinearity is one of the main bottlenecks. As such, it would be rewarding to have already an insight in trajectory optimization for such systems. [41] poses a MATLAB toolbox that can be used to solve trajectory optimization problems. In the toolbox an example can be found on the application of the algorithm on a simplified humanoid robot model. Furthermore, it gives a lot of information on how the solvers work. Nonlinear trajectory optimization methods distinguish themselves between direct and indirect methods, shooting and collocation methods and the difference between the so called ‘h’- and ‘p’-methods. The latter two define the degree of segmentation and the order of used functions between the segments of the problem. Direct collocation methods are most likely best suited for the subject of interest, as they require less computation time than indirect and shooting methods. Using the system description of Eq. (4-2), a direct collocation method could be used for generating a nonlinear trajectory for example.

4-5 Analysis & Discussion

The discussed attempts to use varying CoM height seem interesting, as they differ a lot from each other in how they are derived and used. The E_{orbit} is used for both planning problems and for formulating a MPC that uses varying leg force to come to a stop. By restriction of the z -coordinate to be a function of x , the equations of motion can be integrated in a similar way as in E_{LIP} . This can now be used to relate height trajectories with respect to an ankle position with the state of the CoM. In the MPC approach, this is used to achieve the final goal of ‘capturing’ the CoM above the ankle. The virtual constraint of the function description assumes the direction of motion in x does not change, which might in some cases be or be not be a problem. Another important aspect is that this derivation is done for the 2D side view case. As the authors of [14] describe, virtual constraint approaches are best suited if the degree of underactuation is one. The degree of underactuation in this system is the number of degrees of freedom minus the number of inputs. This corresponds to the number of states minus the leg force, which equals one. In a 3D case integration of the equations of motion might be more challenging and also hard to use for implementation.

The DCM approaches that consider height variation are interesting to make a more in-depth analysis as well. Assumed they all origin from the uncoupled 2D ICP description and thus the LIP orbital energy, a couple of things can be said. Considering the z -coordinate of the state of one of the 3D DCM descriptions, for example Eq. (4-5), the dynamics in the vertical

direction write as

$$\xi_z - z = \sqrt{\frac{z_0}{g}} \dot{z}. \quad (4-8)$$

It rises questions if it is a good assumption that the vertical direction has the same dynamics as the ICP.

Considering the time-varying DCM's xy -components, the ICP and thus E_{LIP} is derived with respect to time, where z is posed to be time-varying. This might be a good approximation for the use in planning or control. Apart from this, with the integration of the LIP equations of motion z is already posed to be constant. The E_{LIP} would look different, and x and z would be coupled, if z would be time varying. The strategies described in [15] give a different perspective on the problem and are inspiring in the sense that also separate strategies can be evaluated, instead of solving a planning problem only.

[39] seems also an interesting approach. Possible concerns are the computation time of the optimization solver and the fact that a walking gait is generated without a predefined footstep plan. The application of [16] gives an alternative method for real-time use, namely that of interpolating between precomputed libraries. Although the dynamics of the robot and the control framework used for it are quite different than those used at IHMC, it is an interesting approach to think about. The fact that the offline trajectories were generated using a direct collocation method, rises also the question if a direct collocation method would be fast enough for the use in a MPC algorithm for example.

Chapter 5

Conclusion

There are numerous ways to describe the dynamical behavior of a walking robot, that are often sufficient for a constant gait over flat terrain. Those assume most of the times a Linear Inverted Pendulum (LIP) model. If there is looked at examples of human behavior by maneuvering over un-flat terrain or during rapid changes in velocity, the constant height assumption might not be always sufficient. With this survey there is an insight gained in the most common robot modeling, planning and control strategies and observed that the height variation of the robot is often not captured in its dynamical description. A selection of one of the most relevant publications concerning this research focus was reviewed, but hardware results are often not shown at robots similar to that in use at IHMC: Atlas or Valkyrie. Furthermore, oftentimes assumptions and constraints were applied to equations, which not have shown yet to give better results than existing models. It seems like an interesting challenge to investigate the effects of height variation in the robot model and to see to what extend this can be applied on a physical robot. The final implementation may have the more complicated shape of a trajectory planning or a Model Predictive Control (MPC) problem, or may use simple heuristics that are implemented in a smart way. In a control problem computation time is an important consideration, and different strategies have to be judged on speed as well.

Bibliography

- [1] “Image of the newest Atlas humanoid robot.” <https://www.bostondynamics.com/atlas#&gid=1&pid=2>. Accessed: 28/07/2018.
- [2] “Image of the Atlas humanoid robot.” <http://robots.ihmc.us/>. Accessed: 28/07/2018.
- [3] “Image of the Valkyrie humanoid robot.” <https://spectrum.ieee.org/automaton/robotics/humanoids/video-friday-ihmc-valkyrie-harvard-arthropods-flying-wheeled-robot>. Accessed: 28/07/2018.
- [4] “Image of the ATRIAS bipedal robot.” <https://mime.oregonstate.edu/research/drl/atrias/>. Accessed: 28/07/2018.
- [5] T. Koolen, S. Bertrand, G. Thomas, T. De Boer, T. Wu, J. Smith, J. Englsberger, and J. Pratt, “Design of a momentum-based control framework and application to the humanoid robot atlas,” *International Journal of Humanoid Robotics*, vol. 13, no. 01, p. 1650007, 2016.
- [6] S. Kajita, T. Yamaura, and A. Kobayashi, “Dynamic walking control of a biped robot along a potential energy conserving orbit,” *IEEE Transactions on robotics and automation*, vol. 8, no. 4, pp. 431–438, 1992.
- [7] J. Pratt, J. Carff, S. Drakunov, and A. Goswami, “Capture point: A step toward humanoid push recovery,” in *Humanoid Robots, 2006 6th IEEE-RAS International Conference on*, pp. 200–207, IEEE, 2006.
- [8] T. Koolen, T. De Boer, J. Rebula, A. Goswami, and J. Pratt, “Capturability-based analysis and control of legged locomotion, part 1: Theory and application to three simple gait models,” *The International Journal of Robotics Research*, vol. 31, no. 9, pp. 1094–1113, 2012.
- [9] S. Kuindersma, R. Deits, M. Fallon, A. Valenzuela, H. Dai, F. Permenter, T. Koolen, P. Marion, and R. Tedrake, “Optimization-based locomotion planning, estimation, and

- control design for the atlas humanoid robot,” *Autonomous Robots*, vol. 40, no. 3, pp. 429–455, 2016.
- [10] J. Chestnutt, M. Lau, G. Cheung, J. Kuffner, J. Hodgins, and T. Kanade, “Footstep planning for the honda asimo humanoid,” in *Robotics and Automation, 2005. ICRA 2005. Proceedings of the 2005 IEEE International Conference on*, pp. 629–634, IEEE, 2005.
 - [11] R. Deits and R. Tedrake, “Footstep planning on uneven terrain with mixed-integer convex optimization,” in *Humanoid Robots (Humanoids), 2014 14th IEEE-RAS International Conference on*, pp. 279–286, IEEE, 2014.
 - [12] J. Englsberger, T. Koolen, S. Bertrand, J. Pratt, C. Ott, and A. Albu-Schäffer, “Trajectory generation for continuous leg forces during double support and heel-to-toe shift based on divergent component of motion,” in *Intelligent Robots and Systems (IROS 2014), 2014 IEEE/RSJ International Conference on*, pp. 4022–4029, IEEE, 2014.
 - [13] M. A. Hopkins, D. W. Hong, and A. Leonessa, “Humanoid locomotion on uneven terrain using the time-varying divergent component of motion,” in *Humanoid Robots (Humanoids), 2014 14th IEEE-RAS International Conference on*, pp. 266–272, IEEE, 2014.
 - [14] T. Koolen, M. Posa, and R. Tedrake, “Balance control using center of mass height variation: limitations imposed by unilateral contact,” in *Humanoid Robots (Humanoids), 2016 IEEE-RAS 16th International Conference on*, pp. 8–15, IEEE, 2016.
 - [15] W. Gao, Z. Jia, and C. Fu, “Increase the feasible step region of biped robots through active vertical flexion and extension motions,” *Robotica*, vol. 35, no. 7, pp. 1541–1561, 2017.
 - [16] Q. Nguyen, A. Agrawal, X. Da, W. C. Martin, H. Geyer, J. W. Grizzle, and K. Sreenath, “Dynamic walking on randomly-varying discrete terrain with one-step preview,” in *Robotics: Science and Systems (RSS)*, 2017.
 - [17] S. Caron, A. Escande, L. Lanari, and B. Mallein, “Capturability-based analysis, optimization and control of 3d bipedal walking,” *arXiv preprint arXiv:1801.07022*, 2018.
 - [18] C. P. Charalambous, “Walking patterns of normal men,” in *Classic Papers in Orthopaedics*, pp. 393–395, Springer, 2014.
 - [19] A. Ramezani, J. W. Hurst, K. A. Hamed, and J. W. Grizzle, “Performance analysis and feedback control of atrias, a three-dimensional bipedal robot,” *Journal of Dynamic Systems, Measurement, and Control*, vol. 136, no. 2, p. 021012, 2014.
 - [20] M. Johnson, B. Shrewsbury, S. Bertrand, T. Wu, D. Duran, M. Floyd, P. Abeles, D. Stephen, N. Mertins, A. Lesman, *et al.*, “Team ihm’s lessons learned from the darpa robotics challenge trials,” *Journal of Field Robotics*, vol. 32, no. 2, pp. 192–208, 2015.
 - [21] N. A. Radford, P. Strawser, K. Hambuchen, J. S. Mehling, W. K. Verdelyen, A. S. Donnan, J. Holley, J. Sanchez, V. Nguyen, L. Bridgwater, *et al.*, “Valkyrie: Nasa’s first bipedal humanoid robot,” *Journal of Field Robotics*, vol. 32, no. 3, pp. 397–419, 2015.

- [22] J. Yamaguchi, E. Soga, S. Inoue, and A. Takanishi, “Development of a bipedal humanoid robot-control method of whole body cooperative dynamic biped walking,” in *Robotics and Automation, 1999. Proceedings. 1999 IEEE International Conference on*, vol. 1, pp. 368–374, IEEE, 1999.
- [23] N. P. Koenig and A. Howard, “Design and use paradigms for gazebo, an open-source multi-robot simulator.,” in *IROS*, vol. 4, pp. 2149–2154, Citeseer, 2004.
- [24] S. Kajita, F. Kanehiro, K. Kaneko, K. Yokoi, and H. Hirukawa, “The 3d linear inverted pendulum mode: A simple modeling for a biped walking pattern generation,” in *Intelligent Robots and Systems, 2001. Proceedings. 2001 IEEE/RSJ International Conference on*, vol. 1, pp. 239–246, IEEE, 2001.
- [25] A. D. Kuo, J. M. Donelan, and A. Ruina, “Energetic consequences of walking like an inverted pendulum: step-to-step transitions,” *Exercise and sport sciences reviews*, vol. 33, no. 2, pp. 88–97, 2005.
- [26] M. Vukobratović and B. Borovac, “Zero-moment point—thirty five years of its life,” *International journal of humanoid robotics*, vol. 1, no. 01, pp. 157–173, 2004.
- [27] P. Sardain and G. Bessonnet, “Forces acting on a biped robot. center of pressure-zero moment point,” *IEEE Transactions on Systems, Man, and Cybernetics-Part A: Systems and Humans*, vol. 34, no. 5, pp. 630–637, 2004.
- [28] M. Vukobratovic and D. Juricic, “Contribution to the synthesis of biped gait,” *IEEE Transactions on Biomedical Engineering*, no. 1, pp. 1–6, 1969.
- [29] M. B. Popovic, A. Goswami, and H. Herr, “Ground reference points in legged locomotion: Definitions, biological trajectories and control implications,” *The International Journal of Robotics Research*, vol. 24, no. 12, pp. 1013–1032, 2005.
- [30] J. Englsberger, C. Ott, and A. Albu-Schäffer, “Three-dimensional bipedal walking control using divergent component of motion,” in *Intelligent Robots and Systems (IROS), 2013 IEEE/RSJ International Conference on*, pp. 2600–2607, IEEE, 2013.
- [31] C. R. Lee and C. T. Farley, “Determinants of the center of mass trajectory in human walking and running.,” *Journal of experimental biology*, vol. 201, no. 21, pp. 2935–2944, 1998.
- [32] R. J. Griffin, G. Wiedebach, S. Bertrand, A. Leonessa, and J. Pratt, “Walking stabilization using step timing and location adjustment on the humanoid robot, atlas,” *arXiv preprint arXiv:1703.00477*, 2017.
- [33] E. R. Westervelt, J. W. Grizzle, and D. E. Koditschek, “Hybrid zero dynamics of planar biped walkers,” 2003.
- [34] H. Asada, Z.-D. Ma, and H. Tokumaru, “Inverse dynamics of flexible robot arms: modeling and computation for trajectory control,” *Journal of dynamic systems, Measurement, and Control*, vol. 112, no. 2, pp. 177–185, 1990.

- [35] S. Kajita, F. Kanehiro, K. Kaneko, K. Fujiwara, K. Harada, K. Yokoi, and H. Hirukawa, “Resolved momentum control: Humanoid motion planning based on the linear and angular momentum,” in *Intelligent Robots and Systems, 2003.(IROS 2003). Proceedings. 2003 IEEE/RSJ International Conference on*, vol. 2, pp. 1644–1650, IEEE, 2003.
- [36] L. Sentis and O. Khatib, “A whole-body control framework for humanoids operating in human environments,” in *Robotics and Automation, 2006. ICRA 2006. Proceedings 2006 IEEE International Conference on*, pp. 2641–2648, IEEE, 2006.
- [37] J. E. Pratt and S. V. Drakunov, “Derivation and application of a conserved orbital energy for the inverted pendulum bipedal walking model,” in *Robotics and Automation, 2007 IEEE International Conference on*, pp. 4653–4660, IEEE, 2007.
- [38] T. Takenaka, T. Matsumoto, and T. Yoshiike, “Real time motion generation and control for biped robot-1 st report: Walking gait pattern generation,” in *Intelligent Robots and Systems, 2009. IROS 2009. IEEE/RSJ International Conference on*, pp. 1084–1091, IEEE, 2009.
- [39] Y. Liu, P. M. Wensing, D. E. Orin, and Y. F. Zheng, “Trajectory generation for dynamic walking in a humanoid over uneven terrain using a 3d-actuated dual-slip model,” in *Intelligent Robots and Systems (IROS), 2015 IEEE/RSJ International Conference on*, pp. 374–380, IEEE, 2015.
- [40] R. Tedrake, I. R. Manchester, M. Tobenkin, and J. W. Roberts, “Lqr-trees: Feedback motion planning via sums-of-squares verification,” *The International Journal of Robotics Research*, vol. 29, no. 8, pp. 1038–1052, 2010.
- [41] M. Kelly, “An introduction to trajectory optimization: how to do your own direct collocation,” *SIAM Review*, vol. 59, no. 4, pp. 849–904, 2017.

Glossary

List of Acronyms

ICP	Instantaneous Capture Point
CP	Capture Point
DCM	Divergent Component of Motion
ZMP	Zero Moment Point
CoP	Center of Pressure
CoM	Center of Mass
CMP	Centroidal Momentum Pivot
eCMP	enhanced Centroidal Momentum Pivot
VRP	Virtual Repellent Point
LIP	Linear Inverted Pendulum
2D	Two-Dimensional Space
3D	Three-Dimensional Space
HZD	Hybrid Zero Dynamics
E_{LIP}	LIP Orbital Energy
E_{orbit}	Nonlinear Orbital Energy
MPC	Model Predictive Control
GUI	Graphical User Interface
SCS	Simulation Construction Set
IMU	Inertial Measurement Unit

EKF Extended Kalman Filter

SLIP Spring-Loaded Inverted Pendulum